

# Choroidal Thickness in Myopic and Nonmyopic Children Assessed With Enhanced Depth Imaging Optical Coherence Tomography

Scott A. Read, Michael J. Collins, Stephen J. Vincent, and David Alonso-Caneiro

Contact Lens and Visual Optics Laboratory, School of Optometry and Vision Science, Queensland University of Technology, Brisbane, Queensland, Australia

Correspondence: Scott A. Read, Contact Lens and Visual Optics Laboratory, School of Optometry and Vision Science, Queensland University of Technology, Room D517, O Block, Victoria Park Road, Kelvin Grove 4059, Brisbane, QLD, Australia; sa.read@qut.edu.au.

Submitted: July 8, 2013

Accepted: October 20, 2013

Citation: Read SA, Collins MJ, Vincent SJ, Alonso-Caneiro D. Choroidal thickness in myopic and nonmyopic children assessed with enhanced depth imaging optical coherence tomography. *Invest Ophthalmol Vis Sci*. 2013;54:7578-7586. DOI:10.1167/iov.13-12772

**PURPOSE.** We examined choroidal thickness (ChT) and its topographic variation across the posterior pole in myopic and nonmyopic children.

**METHODS.** A total of 104 children aged 10 to 15 years (mean age,  $13.1 \pm 1.4$  years) had ChT measured using enhanced depth imaging optical coherence tomography (OCT). Of these children 40 were myopic (mean spherical equivalent,  $-2.4 \pm 1.5$  diopters [D]) and 63 were nonmyopic (mean,  $+0.3 \pm 0.3$  D). Two series of 6 radial OCT line scans centered on the fovea were assessed for each child. Subfoveal ChT and ChT across a series of parafoveal zones over the central 6 mm of the posterior pole were determined through manual image segmentation.

**RESULTS.** Subfoveal ChT was significantly thinner in myopes (mean,  $303 \pm 79 \mu\text{m}$ ) compared to nonmyopes (mean,  $359 \pm 77 \mu\text{m}$ ,  $P < 0.0001$ ). Multiple regression analysis revealed refractive error ( $r = 0.39$ ,  $P < 0.001$ ) and age ( $r = 0.21$ ,  $P = 0.02$ ) were associated positively with subfoveal ChT. Also, ChT exhibited significant topographic variations, with the choroid being thicker in more central regions. The thinnest choroid was observed typically in nasal (mean,  $286 \pm 77 \mu\text{m}$ ) and inferior-nasal ( $306 \pm 79 \mu\text{m}$ ) locations, and the thickest in superior ( $346 \pm 79 \mu\text{m}$ ) and superior-temporal ( $341 \pm 74 \mu\text{m}$ ) locations. The difference in ChT between myopic and nonmyopic children was significantly greater in central foveal regions compared to more peripheral regions ( $>3$  mm diameter,  $P < 0.001$ ).

**CONCLUSIONS.** Myopic children have significantly thinner choroids compared to nonmyopic children of similar age, particularly in central foveal regions. The magnitude of difference in choroidal thickness associated with myopia appears greater than would be predicted by a simple passive choroidal thinning with axial elongation.

Keywords: choroid, refractive error, myopia, pediatric

There is substantial evidence from research with animal models<sup>1-6</sup> and humans<sup>7-16</sup> that the development of refractive errors is associated with changes in the structural characteristics of the choroid. Studies from a range of different animal species, including chicks,<sup>1,2</sup> macaque monkeys,<sup>3</sup> and marmosets,<sup>4</sup> indicate that alterations in choroidal thickness can precede and accompany the development of myopic and hyperopic refractive errors. When experimental myopia is induced in young animals with either negative spectacle lenses (that impose hyperopic defocus) or through the deprivation of form vision, the initial response to this treatment involves a rapid thinning of the choroid, followed by an increase in eye growth.<sup>1-4</sup> Conversely, if hyperopic refractive errors are induced experimentally with positive powered lenses (myopic defocus), then a rapid increase in choroidal thickness followed by a slowing of eye growth typically is observed.<sup>1-4</sup> Pharmacologic treatments, such as dopaminergic agonists<sup>5</sup> and antimuscarinic agents,<sup>6</sup> that inhibit eye growth in chicks also have been shown to result in a transient thickening of the choroid.

Recent cross-sectional studies utilizing optical coherence tomography (OCT) to image and measure the choroid in adult

human subjects with normal ocular health (ages ranging from 19-93 years), have demonstrated that, along with age, refractive error is one of the major factors influencing choroidal thickness.<sup>7-11</sup> These studies, examining adults with diverse refractive errors (ranging from +7 to -20 diopters [D]), with the majority of eyes exhibiting refractive errors between +3 and -3 D) typically have noted choroidal thickness to be thinner in myopic adults compared to emmetropes, and to be thicker in hyperopic adults.<sup>7-11</sup> Studies investigating choroidal thickness in adults with high levels of myopia ( $\geq 6$  D) have reported marked choroidal thinning in these individuals, and it has been postulated that these changes may be a contributing factor to retinal pathology and vision loss associated with high myopia.<sup>12-16</sup>

Although myopia sometimes can begin in adulthood,<sup>17,18</sup> it develops and progresses most commonly in childhood.<sup>19,20</sup> Therefore, examining choroidal thickness and myopia in a pediatric population may provide further insights into the potential role of the choroid in human refractive error development, since this provides an assessment of choroidal characteristics closer to the time that refractive errors, such as myopia, most commonly develop and progress.<sup>19,20</sup> A small

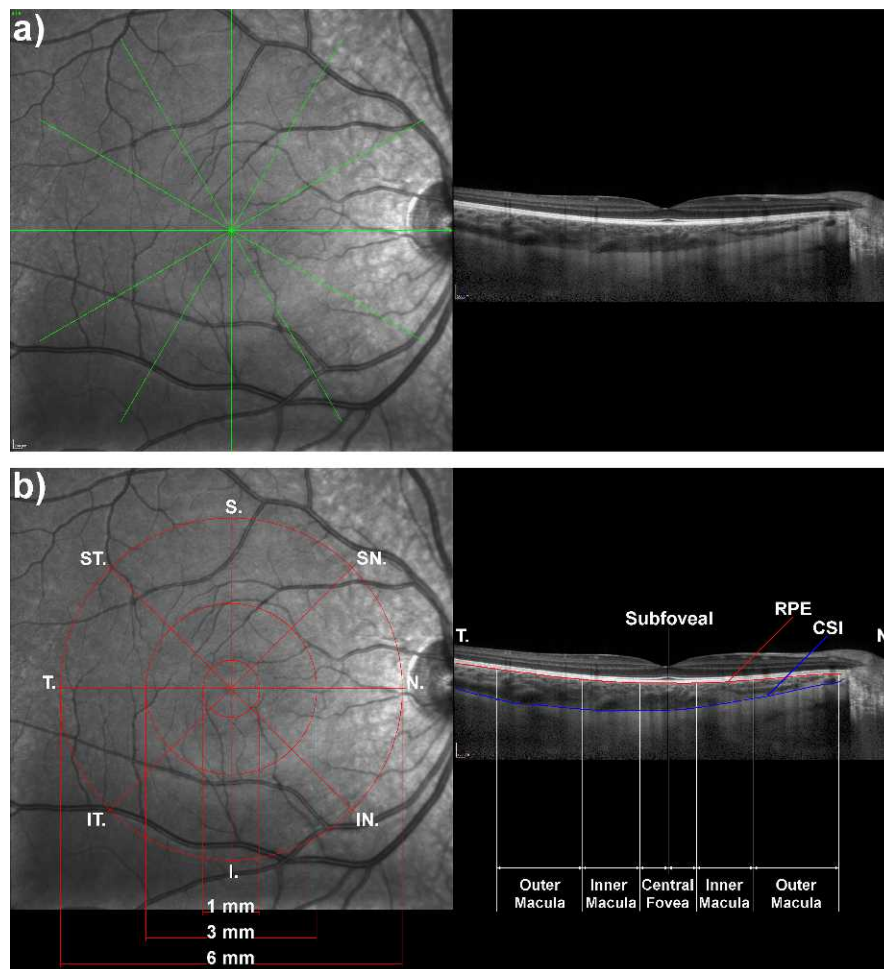


**FIGURE 1.** Overview of the (a) scanning protocol and (b) analysis procedure used in the study. Each child had two series of six radial OCT scan line images captured (position of scans illustrated with green lines in [a]), with each scan line separated by 30° and centered on the fovea (example OCT image from the horizontal scan line is included on the right hand side). Following image capture, each OCT scan was analyzed with custom written software to define the outer border of the RPE (using an automated analysis method) and the inner border of the CSI (performed manually by an experienced masked observer). The thickness data derived from the analysis of each of the six scan lines were analyzed to derive the average choroidal thickness subfoveally, and across a series of locations (temporal [T], superior-temporal [ST], superior [S], superior-nasal [SN], nasal [N], inferior-nasal [IN], inferior [I], and inferior-temporal [IT]) in the central foveal zone (from foveal center out to a 1-mm diameter), the inner macula zone (from inner 1-mm diameter to outer 3-mm diameter), and the outer macula zone (from inner 3-mm diameter to outer 6-mm diameter).

number of recent studies have used OCT imaging to examine choroidal thickness in pediatric subjects.<sup>21–24</sup> However, these studies either have not included participants with significant refractive errors,<sup>23</sup> or have included only limited numbers of myopic children.<sup>21,22,24</sup> Therefore, in our study, we aimed to examine the thickness of the choroid and its topographic variation across the posterior pole in a pediatric population that included a substantial number of myopic children.

## METHODS

### Subjects and Procedures

A total of 104 children aged between 10 and 15 years (mean age  $\pm$  SD, 13.1  $\pm$  1.4 years) participated in this study. Approval from the Queensland University of Technology human research ethics committee was obtained before commencement of the study, and written informed consent was provided by all participating children and their parents. All participants were treated in accordance with the tenets of the Declaration of Helsinki. Before enrollment in the study, all

children underwent an ophthalmic screening examination to determine their visual acuity, noncycloplegic manifest subjective refraction, and ocular health status. All children enrolled in the study had best corrected visual acuity in both eyes of 0.00 logMAR or better; no evidence of amblyopia or strabismus; no evidence or history of significant ocular disease, surgery, or injury; and all reported to be in good general health. No children wore rigid contact lenses (including orthokeratology), and none were under current myopia control treatment (e.g., progressive addition lenses, atropine, and so forth). Four children reported wearing soft disposable contact lenses, but were instructed to remove their lenses on the day of the examination.

Participants were classified based upon the subjective, noncycloplegic spherical equivalent refractive error (SEQ) of their right eye as being myopic (SEQ of  $-0.75$  or less) or nonmyopic (SEQ between  $+1.00$  and  $-0.50$ ). There were 41 subjects classified as myopes (mean SEQ,  $-2.39 \pm 1.51$  D) and 63 as nonmyopes (mean SEQ,  $+0.33 \pm 0.31$  D). The mean cylindrical refraction was  $-0.39 \pm 0.49$  D in the myopes and  $-0.10 \pm 0.21$  D in the nonmyopes. The two groups of children were well matched for age (mean age of the myopes was 13.0

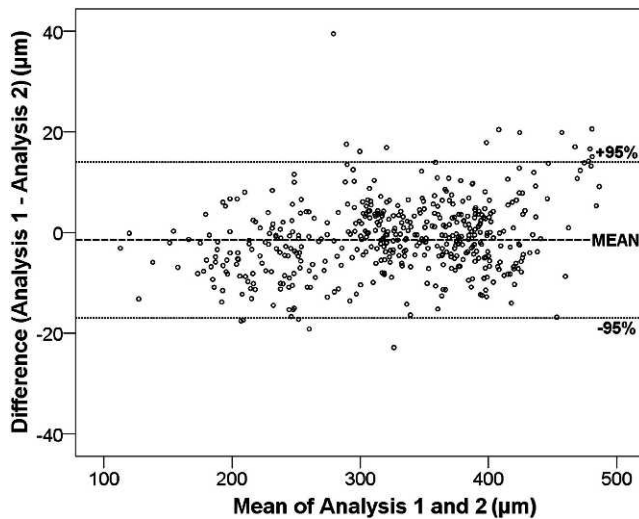


FIGURE 2. Overview of repeatability analysis for subfoveal and parafoveal choroidal thickness measures from the 20 randomly selected subjects that had their scans analyzed twice by the masked observer. The mean of analyses 1 and 2 is plotted against the difference between analyses 1 and 2 (mean difference and 95% limits of agreement are shown with the *dashed lines*).

$\pm 1.5$  years and of the nonmyopes was  $13.1 \pm 1.2$  years) and sex (the myopic and nonmyopic populations consisted of 49% and 46% male children, respectively). All children classified as myopes exhibited unaided visual acuity of 0.06 logMAR or worse, and all previously had been prescribed distance refractive corrections that were worn on either a part-time or full-time basis.

All measurements were carried out between 2 and 5 PM to limit the potential confounding influence of diurnal variations in choroidal thickness.<sup>25,26</sup> Following the initial screening examination, each child had spectral domain OCT chorioretinal images of their right eye captured using the Heidelberg Spectralis instrument (Heidelberg Engineering, Heidelberg, Germany). The Heidelberg Spectralis device uses a super luminescent diode of central wavelength 870 nm for OCT imaging, with an axial resolution of 3.9  $\mu\text{m}$  and transverse resolution of 14  $\mu\text{m}$  in retinal tissue, and a scanning speed of 40,000 A-scans per second. For each participating child, two series of six radial OCT scan lines, each separated by 30° and centered on the fovea, were captured using the instrument's Enhanced Depth Imaging (EDI) mode. The EDI mode focuses the instrument closer to the posterior eye than the standard

imaging mode to enhance the visibility of the choroid in the OCT scans.<sup>27</sup> The instrument's automatic real-time eye tracking function was utilized and each radial OCT image was the average of 30 scans. Each scan line was 30° long and was captured using the instrument's high resolution scanning protocol, which results in a B-scan image consisting of 1536  $\times$  496 pixels. Figure 1a illustrates the scanning protocol used, with an example OCT image from a representative subject. Consistent with previous pediatric retinal imaging studies,<sup>28</sup> only scans with quality index (QI) values greater than 20 dB were included for analysis (the mean QI from all measurements was  $33 \pm 3$  dB). A small number of children ( $n = 5$ , 3 nonmyopes and 2 myopes) were unable to maintain stable fixation for long enough to allow all six radial scan lines to be captured, and so a single horizontal scan image (the average of 30 B-scans) centered on the fovea was collected and analyzed for these subjects. Each child also had their ocular dimensions (including central corneal thickness, anterior chamber depth, lens thickness, and axial length) measured using an optical biometer (Lenstar LS 900; Haag Streit AG, Koeniz, Switzerland) based upon the principles of optical low coherence reflectometry.<sup>29</sup>

### Data Analysis

Following data collection, the OCT images were exported from the instrument and analyzed using custom written software. Each of the two sets of scans for each subject were analyzed to segment the outer surface of the RPE, and the inner surface of the choriocleral interface (CSI), to determine choroidal thickness across the 30° width of each scan. The RPE initially was segmented using an automated method based on graph theory.<sup>30</sup> An experienced masked observer then manually segmented the CSI using a method that has been described in detail previously,<sup>23</sup> and involves the observer manually selecting a series of points along the CSI. The software then automatically fits a smooth function (spline fit) to these points to define the boundary. Additionally, the observer also checked the integrity of the automated segmentation of the RPE and manually corrected any segmentation errors. The center of the fovea, defined as the deepest point in the central foveal pit, also was marked in each scan by the observer.

Following the segmentation of the OCT scans, the choroidal thickness data from each scan had the transverse scaling corrected to account for ocular magnification effects, based upon each participant's biometric and refraction measurements. The length in millimeters of each 30° scan was determined based upon the distance from the retina to the eye's second nodal point, assuming a spherical retina.<sup>31</sup> The position of the second nodal point for each individual subject

TABLE 1. Overview of Mean  $\pm$  SD Subfoveal Choroidal Thickness (Derived From the Spectralis OCT Images), Ocular Biometric Measures (From the Lenstar Optical Biometer), and Refractive Error (Derived From a Noncycloplegic Manifest Subjective Refraction) in the Myopic and Nonmyopic Children

	Mean $\pm$ SD Biometric Measure		
	Myopic Subjects, $n = 41$	Nonmyopic Subjects, $n = 63$	All Subjects, $n = 104$
Spherical equivalent refraction, D	$-2.39 \pm 1.51$	$+0.33 \pm 0.31$	$-0.73 \pm 1.65$
Central corneal thickness, $\mu\text{m}$	$543 \pm 27$	$555 \pm 28$	$550 \pm 28$
Anterior chamber depth, mm	$3.33 \pm 0.20$	$3.10 \pm 0.24$	$3.19 \pm 0.25$
Lens thickness, mm	$3.37 \pm 0.15$	$3.52 \pm 0.19$	$3.46 \pm 0.19$
Vitreous chamber depth, mm	$17.21 \pm 1.10$	$16.09 \pm 0.65$	$16.53 \pm 1.01$
Axial length, mm	$24.46 \pm 1.07$	$23.26 \pm 0.64$	$23.73 \pm 1.02$
Subfoveal choroidal thickness, $\mu\text{m}$	$303 \pm 79$	$359 \pm 77$	$337 \pm 82$

All ocular measures were significantly different between the myopic and nonmyopic children ( $P < 0.001$ ), except for central corneal thickness ( $P = 0.06$ ).

**TABLE 2.** Overview of the Results From the Stepwise Multiple Regression Analysis Examining the Influence of Demographic and Biometric Predictors of Subfoveal Choroidal Thickness

Predictor Variables	Unstandardized Coefficients	Standardized Coefficients	Significance, <i>P</i> Value
	<i>B</i> (SE)	$\beta$	
Refractive error	19.4 (4.5)	0.39	<0.001
Age	13.1 (5.5)	0.21	0.02

The final regression model had an  $r^2$  of 0.18 ( $P < 0.0001$ ).

was determined with the “step along” method,<sup>32</sup> using each subject’s measured ocular refraction and ocular biometry measures, applying the methods outlined by Bennett<sup>33</sup> to determine the equivalent power of the eye and crystalline lens.

The thickness data subsequently was analyzed to determine the subfoveal choroidal thickness, and the average choroidal thickness across a series of concentric zones around the fovea, including the central foveal zone (central 1-mm diameter), the inner macula zone (from an inner diameter of 1 mm to an outer diameter of 3 mm), and the outer macula zone (inner diameter of 3 mm and outer diameter of 6 mm, Fig. 1b). This analysis provided the average thickness at 8 locations (temporal, superior-temporal, superior, superior-nasal, nasal, inferior-nasal, inferior, and inferior-temporal), across each of the three zones (central fovea, inner macula, and outer macula).

To assess the reliability and repeatability of the thickness data derived from the manual segmentation of the OCT images, the scans from 20 randomly selected subjects were analyzed twice by the observer, who was masked to the choroidal thickness results from the initial analysis. The subfoveal and parafoveal (central fovea, inner macula, and outer macula zones) thickness data were analyzed using the methods described by Bland and Altman.<sup>34</sup> Since there appeared to be a trend for the differences between the two analyses to be slightly greater for thicker choroids, the mean differences and limits of agreement were determined based upon the ratios of the differences between the two analyses.<sup>34</sup>

The influence of refractive error and sex upon subfoveal choroidal thickness was examined with a 2-way ANOVA. Additionally, a stepwise multiple regression was performed to examine the influence of demographic (age and sex) and biometric ocular factors (spherical equivalent refractive error, axial length, central corneal thickness, anterior chamber depth, and lens thickness) upon the subfoveal choroidal thickness measures. To examine the topographic distribution of choroidal thickness across the posterior pole, a repeated measures ANOVA was performed with two within-subjects factors, including choroidal location (temporal, superior-temporal, superior, superior-nasal, nasal, inferior-nasal, inferior, or inferior-temporal) and choroidal zone (central foveal, inner macula, and outer macula), and one between-subjects factor (refractive error group). The five children who exhibited poor fixation during OCT imaging were excluded from the topographic analysis of choroidal thickness. All results presented represent the mean  $\pm$  SD.

## RESULTS

### Observer Repeatability

Bland-Altman<sup>34</sup> analysis of intraobserver repeatability for the 20 scans that were analyzed twice by the observer revealed excellent repeatability for the determination of subfoveal and parafoveal choroidal thickness, comparable with previous reports of intraobserver repeatability.<sup>35</sup> Repeatability was similar for the subfoveal and parafoveal measures, so these were considered together. Choroidal thickness from the two repeated analyses appeared to agree closely, with the mean difference being smaller than the axial resolution of the instrument. The mean and 95% limits of agreement for the difference between the 2 repeated analyses of choroidal thickness was  $-1.6 \pm 7.9 \mu\text{m}$  (95% limits of agreement,  $+14.1$  to  $-17.2 \mu\text{m}$ ). Figure 2 illustrates the agreement between the two analyses. The differences between the two repeated analyses exhibited a trend to be slightly larger for thicker choroids.

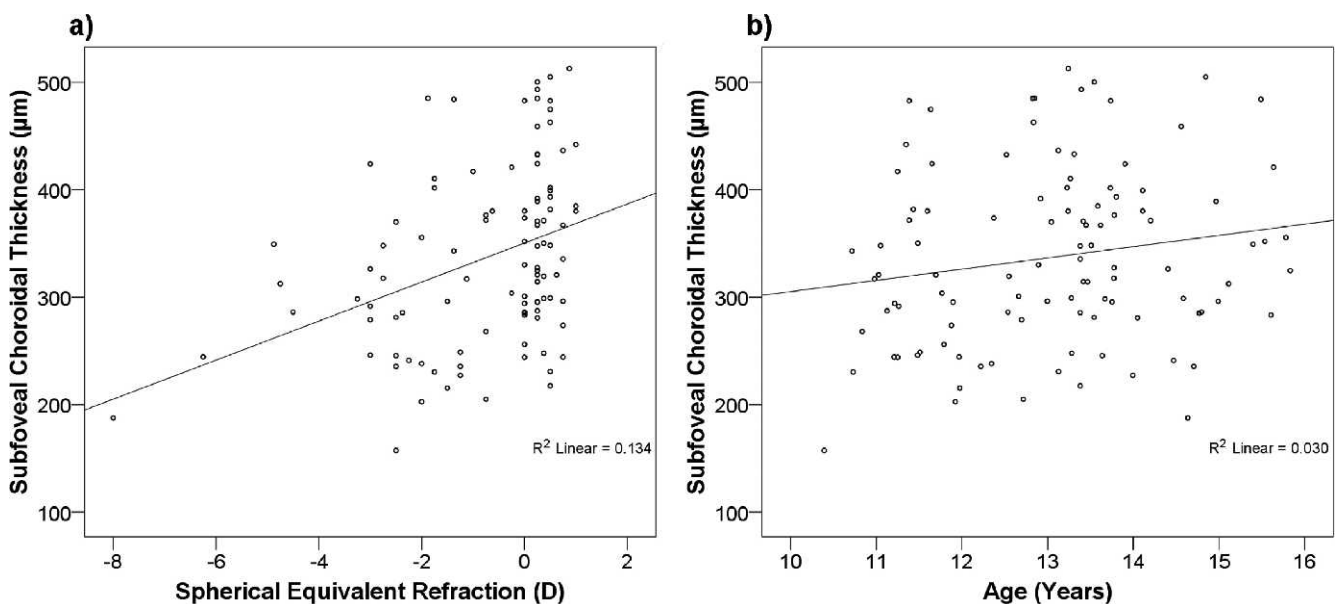


**FIGURE 3.** Association between subfoveal choroidal thickness and refractive error (a), and subfoveal choroidal thickness and age (b) for the population of 104 children examined. Multiple regression analysis revealed that noncycloplegic spherical equivalent refraction ( $P < 0.001$ ) and age ( $P = 0.02$ ) were significantly associated with subfoveal choroidal thickness.

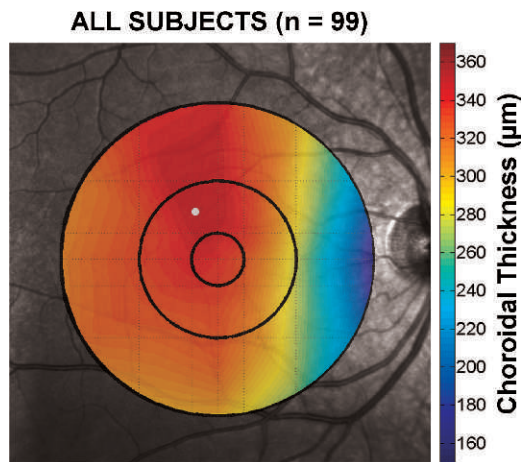


**FIGURE 4.** Average topographic distribution of choroidal thickness across the central 6 mm of the posterior pole for all children with complete sets of six OCT images in the study ( $n = 99$ ). White spot indicates the average position of the thickest choroid. Thickness map represents the mean choroidal thickness of all subjects; however, fundus image background is from one representative subject to illustrate the location of the choroidal thickness measurements in relation to typical fundus landmarks. Circles indicate the position of the central foveal zone (inner 1-mm), inner macula zone (from inner 1-mm to outer 3-mm diameter), and outer macula zone (from inner 3-mm to outer 6-mm diameter).

### Subfoveal Choroidal Thickness

The average subfoveal choroidal thickness, along with an overview of the other ocular biometric measures is presented in Table 1. The myopic children (mean subfoveal choroidal thickness,  $303 \pm 79 \mu\text{m}$ ) exhibited a significantly thinner subfoveal choroid than the nonmyopic children (mean,  $359 \pm 77 \mu\text{m}$ ;  $P < 0.001$ ). No significant effect of sex was found on the subfoveal choroidal thickness measures ( $P = 0.77$ ) and there was no significant refractive error by sex interactions ( $P > 0.05$ ). Most of the other measured ocular biometrics examined (Table 1) also exhibited significant differences associated with refractive error, except for central corneal thickness ( $P > 0.05$ ). Myopic children exhibited deeper anterior chambers (mean difference, 0.24 mm;  $P < 0.001$ ), thinner crystalline lenses (mean difference, 0.15 mm;  $P < 0.001$ ), and longer vitreous chambers (mean difference, 1.12 mm;  $P < 0.001$ ) and axial lengths (mean difference, 1.20 mm;  $P < 0.001$ ) compared to the nonmyopic children. The largest differences between myopes and nonmyopes were found in terms of axial length and vitreous chamber depth, confirming an axial origin of the myopia.

Stepwise multiple regression analysis revealed that refractive error and age were significant predictors of subfoveal choroidal thickness (Table 2, Fig. 3). The regression model was highly statistically significant ( $P < 0.001$ ), with a correlation  $r^2$  of 0.18. Of the significant predictor variables, refractive error exhibited a significant positive association (slope,  $+19.4 \mu\text{m}/\text{D}$ ), and appeared to have the strongest relationship with subfoveal choroidal thickness (including refractive error in the model increased the  $r^2$  of the model by 0.13,  $P < 0.001$ ). Age exhibited a significant positive association (slope,  $+13.1 \mu\text{m}/\text{y}$ ) with subfoveal choroidal thickness, and its inclusion in the model increased the  $r^2$  by 0.05 ( $P = 0.02$ ). Univariate analyses revealed a significant negative association between axial length ( $r = -0.306$ , slope =  $-0.004$ ,  $P = 0.002$ ) and vitreous chamber depth ( $r = -0.310$ , slope =  $-0.004$ ,  $P = 0.001$ ) with subfoveal choroidal thickness, but these predictors were not significant in the final multiple regression model due to the substantial

colinearity between axial length, vitreous chamber depth, and refractive error.

To explore the potential mechanism underlying the thinner choroid observed in the myopic children, we used a similar approach to that described by Troilo et al.,<sup>4</sup> modeling the choroid as an isovolumetric shell of a sphere to estimate the predicted change in choroidal thickness that would occur based upon a passive stretch due to the longer axial length of the myopic children. This modeling estimated that the measured average difference in axial length between the myopic and nonmyopic children (1.2 mm) would lead to a 21- $\mu\text{m}$  thinner choroid in the myopic children (based upon passive stretch alone), which is substantially less than the measured 56- $\mu\text{m}$  thinner subfoveal choroid in the myopic children. We also examined the choroidal thickness of a subset of nonmyopic children with longer axial lengths than average (24 mm or greater) and for these six children with a mean axial length of  $24.46 \pm 0.36$  mm, a mean subfoveal choroidal thickness of  $401 \pm 98 \mu\text{m}$  was found ( $\sim 98 \mu\text{m}$  thicker than the 41 myopic children who also had a mean axial length of 24.46 mm). These findings suggested that mechanisms additional to a simple passive stretch are involved in the differences observed between the myopic and nonmyopic children.

### Topographic Choroidal Thickness

Figure 4 and Table 3 illustrate the topographic distribution of choroidal thickness across the central 6 mm of the posterior pole for all subjects with complete sets of OCT images (39 myopes and 60 nonmyopes). Significant changes were observed in choroidal thickness as a function of topographic zone, with the central foveal zone (mean thickness,  $339 \pm 82 \mu\text{m}$ ) being significantly thicker than the inner macula zone ( $330 \pm 78 \mu\text{m}$ ), and the outer macula zone ( $302 \pm 66 \mu\text{m}$ ,  $P < 0.001$  for all comparisons). Choroidal thickness also changed significantly with measurement location, with the thinnest choroid observed in the nasal (mean of all zones,  $286 \pm 77 \mu\text{m}$ ) and inferior-nasal ( $306 \pm 79 \mu\text{m}$ ) locations, and the thickest choroid in the superior ( $346 \pm 79 \mu\text{m}$ ) and superior-temporal ( $341 \pm 74 \mu\text{m}$ ) locations. A significant choroidal location by zone interaction was observed, as the rate of change in choroidal thickness from central to more peripheral zones varied with location. For the superior and superior-temporal locations, choroidal thickness did not change significantly between the central foveal and outer macula zones ( $P > 0.05$ ), whereas the outer macula zone was significantly thinner than the central foveal zone for all other locations ( $P < 0.05$  for all comparisons).

Significant differences in choroidal thickness across the posterior pole associated with refractive error also were found (Table 3, Fig. 5). For all zones and locations considered together, on average the choroid was significantly thinner in the myopic children (mean,  $294 \pm 71 \mu\text{m}$ ) compared to the nonmyopic children (mean,  $343 \pm 71 \mu\text{m}$ ;  $P < 0.001$ ). Pairwise comparisons revealed the myopic children to have significantly thinner choroids at each of the measured locations ( $P < 0.05$  for all comparisons). A significant measurement zone by refraction interaction also was observed ( $P < 0.001$ ), due to the difference in thickness between the myopic and nonmyopic children being greater in more central compared to the more peripheral zones (the choroid of the myopic children was 58  $\mu\text{m}$  thinner than that of the nonmyopic children in the central foveal zone, compared to 37  $\mu\text{m}$  thinner in the outer macula zone). This difference indicated a greater rate of choroidal thinning from central to more peripheral zones in the nonmyopic (mean difference,  $44 \pm 26 \mu\text{m}$  between the central foveal zone and the outer macula zone) compared to the myopic children (mean difference,  $23 \pm 24 \mu\text{m}$ ;  $P <$

**TABLE 3.** Overview of the Mean  $\pm$  SD Parafoveal Choroidal Thickness Measures in the Central Foveal, Inner Macula and Outer Macula Zones in the Myopic ( $n = 39$ ), Nonmyopic ( $n = 60$ ), and All Children ( $n = 99$ ) With Complete Choroidal Thickness Data From All Six Radial Scan Lines

	Mean $\pm$ SD Choroidal Thickness, $\mu\text{m}$			
	Foveal Zone	Inner Macula Zone	Outer Macula Zone	All Zones
<b>Temporal</b>				
Myopes, $n = 39$	308 $\pm$ 78	312 $\pm$ 79	305 $\pm$ 77	308 $\pm$ 77
Nonmyopes, $n = 60$	362 $\pm$ 76	354 $\pm$ 69	336 $\pm$ 61	351 $\pm$ 66
All subjects, $n = 99$	341 $\pm$ 81	337 $\pm$ 76	324 $\pm$ 69	334 $\pm$ 73
<b>Superior-temporal</b>				
Myopes, $n = 39$	309 $\pm$ 78	317 $\pm$ 77	318 $\pm$ 73	315 $\pm$ 74
Nonmyopes, $n = 60$	365 $\pm$ 77	362 $\pm$ 72	345 $\pm$ 66	358 $\pm$ 69
All subjects, $n = 99$	343 $\pm$ 82	345 $\pm$ 77	335 $\pm$ 70	341 $\pm$ 74
<b>Superior</b>				
Myopes, $n = 39$	306 $\pm$ 76	314 $\pm$ 74	318 $\pm$ 76	313 $\pm$ 74
Nonmyopes, $n = 60$	364 $\pm$ 78	371 $\pm$ 78	367 $\pm$ 76	367 $\pm$ 76
All subjects, $n = 99$	342 $\pm$ 82	348 $\pm$ 81	348 $\pm$ 79	346 $\pm$ 79
<b>Superior-nasal</b>				
Myopes, $n = 39$	302 $\pm$ 78	294 $\pm$ 75	262 $\pm$ 63	286 $\pm$ 71
Nonmyopes, $n = 60$	362 $\pm$ 79	352 $\pm$ 82	305 $\pm$ 80	340 $\pm$ 79
All subjects, $n = 99$	338 $\pm$ 84	329 $\pm$ 84	288 $\pm$ 76	319 $\pm$ 80
<b>Nasal</b>				
Myopes, $n = 39$	297 $\pm$ 76	269 $\pm$ 71	199 $\pm$ 58	255 $\pm$ 67
Nonmyopes, $n = 60$	357 $\pm$ 79	327 $\pm$ 82	232 $\pm$ 77	305 $\pm$ 76
All subjects, $n = 99$	333 $\pm$ 83	304 $\pm$ 83	219 $\pm$ 72	286 $\pm$ 77
<b>Inferior-nasal</b>				
Myopes, $n = 39$	298 $\pm$ 79	280 $\pm$ 77	245 $\pm$ 69	274 $\pm$ 74
Nonmyopes, $n = 60$	358 $\pm$ 79	338 $\pm$ 79	283 $\pm$ 73	326 $\pm$ 76
All subjects, $n = 99$	335 $\pm$ 83	315 $\pm$ 83	268 $\pm$ 73	306 $\pm$ 79
<b>Inferior</b>				
Myopes, $n = 39$	301 $\pm$ 79	299 $\pm$ 79	293 $\pm$ 66	298 $\pm$ 73
Nonmyopes, $n = 60$	360 $\pm$ 78	353 $\pm$ 76	333 $\pm$ 70	349 $\pm$ 73
All subjects, $n = 99$	337 $\pm$ 83	331 $\pm$ 81	318 $\pm$ 71	329 $\pm$ 77
<b>Inferior-temporal</b>				
Myopes, $n = 39$	304 $\pm$ 78	303 $\pm$ 77	299 $\pm$ 71	302 $\pm$ 75
Nonmyopes, $n = 60$	361 $\pm$ 77	353 $\pm$ 72	335 $\pm$ 68	350 $\pm$ 71
All subjects, $n = 99$	339 $\pm$ 82	333 $\pm$ 78	321 $\pm$ 71	331 $\pm$ 76

Pairwise comparisons between myopes and nonmyopes revealed significant differences between refractive error groups at all locations ( $P < 0.05$ ).

0.001). This is illustrated further in Figure 5b, which shows the topographic distribution of the average difference in choroidal thickness between myopes and nonmyopes across the central posterior pole. There was no significant location by refraction interaction ( $P = 0.2$ ), suggesting the differences between the myopic and nonmyopic children were similar for the eight different locations that were assessed.

## DISCUSSION

Our study demonstrated that myopic children have significantly thinner choroids (on average by 50  $\mu\text{m}$ ) compared to nonmyopic children of similar age. Previous studies of choroidal thickness in childhood either have not included subjects with significant refractive error,<sup>23</sup> or have included only small numbers of myopic participants,<sup>21,22,24</sup> which has precluded a detailed examination of the influence of myopia upon choroidal thickness in childhood. A thinning of the choroid associated with myopia has been demonstrated in a number of studies examining adult subjects<sup>7-11</sup>; however, to our knowledge ours is the first study to confirm this finding in a substantial population of pediatric subjects. A thinner choroid in adults with myopia, and particularly the marked choroidal thinning reported in highly myopic adults,<sup>12-16</sup> provides evidence that a thinning of the choroid is a long-term correlate of myopic axial elongation of the eye. Since myopia typically begins in childhood, our findings suggested that choroidal thinning occurs relatively early in the refractive error development process. A thinner choroid in childhood myopia also is consistent qualitatively with animal research that reports choroidal thinning associated with experimental manipulations resulting in increased eye growth and the development of myopia in young animals.<sup>1-4</sup>

Although further research is required to understand better the exact mechanism underlying the thinner choroid observed in myopic children, the magnitude of the difference that we have observed between myopes and nonmyopes appears to be greater than would be explained by a simple mechanical stretch of choroidal tissue with axial elongation. The subfoveal choroid of the myopic children was, on average, 16% thinner than that of the nonmyopic children, whereas modeling to estimate the change in choroidal thickness that would occur as a result of passive stretch due to axial elongation in the myopic children predicted only a 6% thinner choroid. This suggested that other physiological choroidal changes associated with myopia, beyond a simple passive stretch with increasing eye length, also are likely to contribute to the choroidal thickness differences observed. The choroid is a highly vascular structure, so alterations in ocular blood flow or vascular changes associated with myopia also potentially could have a role. A recent study has reported microvascular changes in the retina (narrower arteriolar and venular caliber) of children associated with axial elongation of the eye, suggesting a potential effect of myopia on the microvascular structures of the eye from an early age.<sup>36</sup> Previous studies in animals demonstrate that optical stimuli (i.e., hyperopic defocus or diffuse defocus) can induce choroidal thinning,<sup>1-4</sup> which leaves open the possibility that optical factors (e.g., chronic hyperopic defocus associated with lag of accommodation during near tasks or ocular aberrations) also potentially could contribute to the thinner choroid in myopic children.

Multiple regression analysis revealed that refractive error and age were significantly associated with choroidal thickness in this population, with refractive error appearing to be the stronger predictor. This analysis predicted a decrease in choroidal thickness of 19  $\mu\text{m}$  for each diopter of myopia, and an increase in choroidal thickness of 13.1  $\mu\text{m}$  for every year of

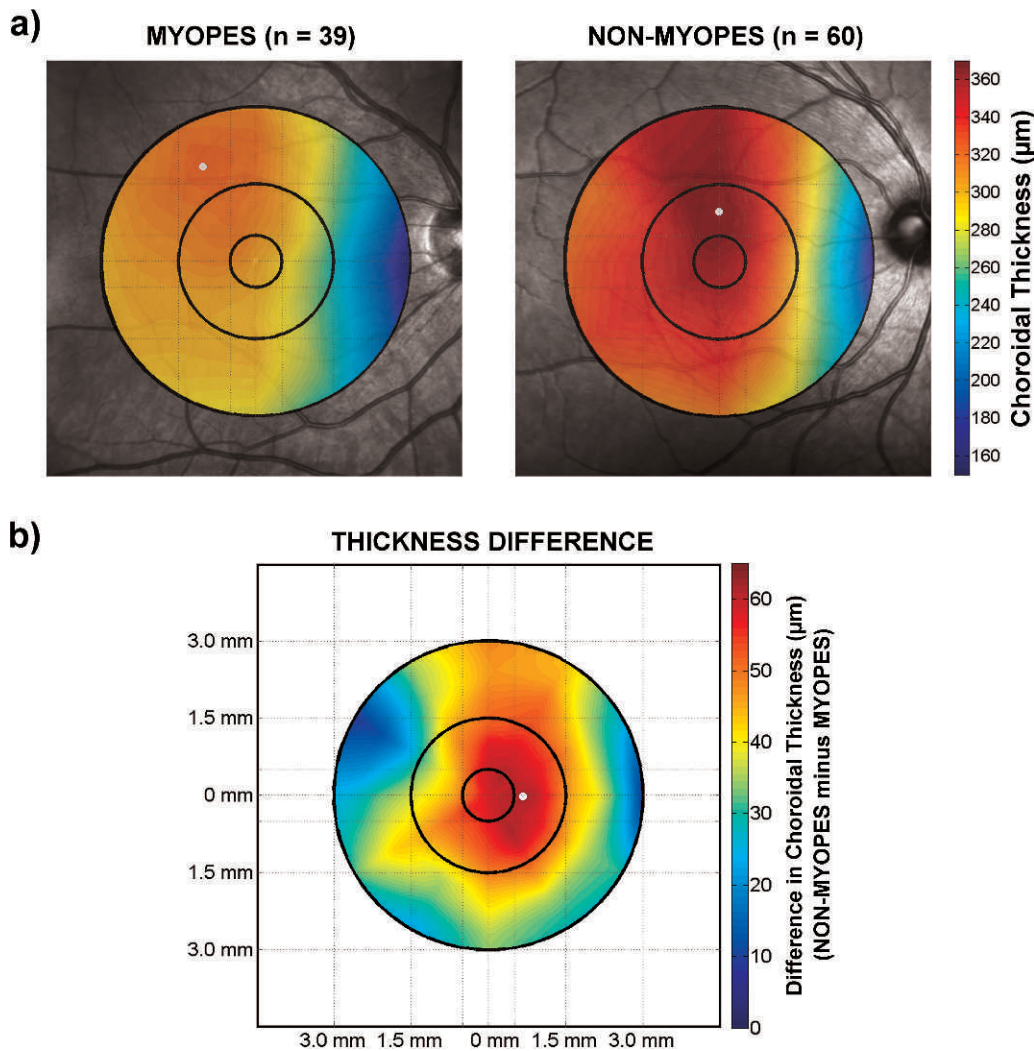


**FIGURE 5.** Average choroidal thickness maps across the central 6 mm of the posterior pole for the myopic ( $n = 39$ ) and nonmyopic ( $n = 60$ ) children with complete sets of six OCT images in the study (a). Thickness maps represent the mean choroidal thickness from all myopic and nonmyopic children respectively; however, the fundus image background is from one representative myopic and nonmyopic child to illustrate the location of the choroidal thickness measurements in relation to typical fundus landmarks. Average difference in choroidal thickness (nonmyopes minus myopes) across the central 6 mm of the posterior pole is illustrated in (b). *White spot* indicates the average position of the thickest choroid (a) and the largest thickness difference (b). *Circles* indicate the position of the central foveal zone (inner 1-mm diameter), inner macula zone (from inner 1-mm to outer 3-mm diameter), and outer macula zone (from inner 3-mm to outer 6-mm diameter).

age. In our previous study<sup>23</sup> examining choroidal thickness in a younger cohort of primarily emmetropic children (aged 4–12 years), we also found evidence of a positive association between age and choroidal thickness, with the younger 4- to 6-year-old children (mean choroidal thickness, 312  $\mu\text{m}$ ) having a thinner choroid than the older cohort examined (mean of 341  $\mu\text{m}$  in the 10–12-year-olds). Our current study, using a different OCT instrument and scanning protocol, found a similar thickness in 10- to 12-year-old nonmyopic children (351  $\mu\text{m}$ ) and extends our previous work by showing that the choroid still appears to be undergoing small increases in thickness associated with age in the teenage years (mean thickness of 365  $\mu\text{m}$  in nonmyopic 13–15-year-olds). In our current study, there was no evidence of a significant age by refractive error interaction, indicating that myopic and nonmyopic children appear to exhibit an increase in choroidal thickness with age. We speculated that this finding, coupled with the overall thinner choroid observed in our myopic children, suggests that myopic children have a thinner choroid

compared to nonmyopic children, even at younger ages and potentially before the development of myopia. It also should be noted that the nonmyopic sample is likely to include a proportion of participants who may have myopia in the future. Further longitudinal measures of choroidal thickness in myopic and nonmyopic children are required to clarify the magnitude and time course of choroidal changes occurring with age, and associated with the development and progression of myopia in childhood.

We also observed significant variations in the topographic distribution of choroidal thickness across the posterior pole. Although our study employed a scanning protocol that sampled a slightly larger area of the choroid than previous studies of pediatric choroidal thickness, our finding of a thinner choroid nasally and inferonasally, and slightly thicker choroid in superior and superior-temporal regions, generally are similar to previous reports of the choroid in childhood.<sup>21–24</sup> A thinner choroid nasally compared to temporally, and a thicker choroid in superior regions compared to inferior also

has been a relatively consistent finding in studies examining the distribution of choroidal thickness across the posterior pole in adult subjects.<sup>7,8,37</sup> These topographic variations in choroidal thickness are likely to be related to regional differences in the metabolic demands of the retina, along with other anatomic factors, such as the pattern of distribution of the choroidal vasculature and position of choroidal watershed zones,<sup>38</sup> and the position of the entrance of the optic nerve in the globe.

A significant refractive error by choroidal region/zone interaction was found, indicating that the change in choroidal thickness from center to more peripheral regions was different between the myopic and nonmyopic children. This manifests itself as a more pronounced difference in choroidal thickness between myopic and nonmyopic children in more central foveal regions. This finding suggests that there are regional differences in the choroidal architecture associated with myopia. The more pronounced difference (i.e., thinner) in choroidal thickness centrally suggests that the central choroid may have a greater capacity to thin than more peripheral regions, either due to mechanical restrictions/influences or the anatomic and physiological characteristics of this region. It has been documented that the human choroid contains a relatively large number of nonvascular smooth muscle cells concentrated in the foveal regions compared to more peripheral regions,<sup>39</sup> and it has been hypothesized that contraction of these cells may be involved in choroidal thinning associated with refractive error development,<sup>40</sup> which potentially could contribute to regionally varying changes in choroidal thickness. If the thickness of the choroid is influenced by signals from the overlying retina, this regional difference in thickness between myopic and nonmyopic children also could indicate that the signal for choroidal change associated with myopia also may vary regionally.

Although the cross-sectional analysis in our current study means we cannot attribute causation to the associations that we found, the thinner choroid observed in the myopic children supports a potential role for the choroid in the development and progression of myopia. Various putative roles for the choroid in the regulation of eye growth have been hypothesized, from the choroid being a source of growth factors that influence the sclera,<sup>41</sup> to the choroid acting as a barrier to diffusion of retinal-derived factors acting on the sclera,<sup>42</sup> to the choroid modulating the tension on the sclera under the influence of ciliary muscle tone.<sup>43</sup> If the thickness of the choroid does influence the movement of growth factors to the sclera, then a thinner choroid would be predicted to be related to an increased growth of the eye and, hence, be associated with the presence of myopia, as we have found in our study. Further research examining longitudinal changes in the choroid in childhood refractive error development is required to further our understanding of the relationship between the thickness of the choroid, and the development and progression of refractive errors in humans.

There is evidence from animal studies,<sup>6</sup> and from a recent study in young adult humans (Sander B, et al. *IOVS* 2013;54:ARVO E-Abstract 5168), that antimuscarinic drugs (such as those used in topical cycloplegic agents) can lead to significant increases in choroidal thickness. Since the exact influence of antimuscarinics on the choroid of myopic and nonmyopic children has not been established, it was decided not to use cycloplegia for the measures in our study to ensure that our choroidal measurements were not confounded by any potential effects of cycloplegics on the choroid. However, the lack of cycloplegia is a limitation of the refractive measures in the study, since this may influence the reliability of refraction measures in pediatric populations.<sup>44</sup> Since all of our myopic participants had clinically established myopic refractive errors,

it is unlikely that the noncycloplegic measures will have led to a misclassification of these subjects. However, it is likely that a cycloplegic refraction would result in a more hyperopic mean refraction in some of our nonmyopic cohort.

## CONCLUSIONS

In conclusion, our study demonstrated a significantly thinner choroid in myopic children compared to nonmyopic children of the same age. The thinner choroid in myopic children appears to be more pronounced in central foveal regions compared to more peripheral regions of the choroid. These findings are consistent with a potential role of the choroid in human refractive error development.

## Acknowledgments

The authors thank Rod Jensen for assistance in the analysis of the OCT images.

Supported by Australian Research Council Discovery Early Career Research Award DE120101434 (SAR).

Disclosure: **S.A. Read**, None; **M.J. Collins**, None; **S.J. Vincent**, None; **D. Alonso-Caneiro**, None

## References

1. Wallman J, Wildsoet C, Xu A, et al. Moving the retina: choroidal modulation of refractive state. *Vision Res.* 1995;35:37-50.
2. Wildsoet CE, Wallman J. Choroidal and scleral mechanisms of compensation for spectacle lenses in chicks. *Vision Res.* 1995;35:1175-1194.
3. Hung LF, Wallman J, Smith EL. Vision-dependant changes in the choroidal thickness of macaque monkeys. *Invest Ophthalmol Vis Sci.* 2000;41:1259-1269.
4. Troilo D, Nickla DL, Wildsoet CE. Choroidal thickness changes during altered eye growth and refractive state in a primate. *Invest Ophthalmol Vis Sci.* 2000;41:1249-1258.
5. Nickla DL, Totonnelly K, Dhillon B. Dopaminergic agonists that result in ocular growth inhibition also elicit transient increases in choroidal thickness in chicks. *Exp Eye Res.* 2012;91:715-720.
6. Nickla DL, Zhu X, Wallman J. Effects of muscarinic agents on chicks choroids in intact eyes and eyecups: evidence for a muscarinic mechanism in choroidal thinning. *Ophthalmic Physiol Opt.* 2013;33:245-256.
7. Esmaeelpour M, Považay B, Hermann B, et al. Three-dimensional 1060-nm OCT: choroidal thickness maps in normal subjects and improved posterior segment visualization in cataract patients. *Invest Ophthalmol Vis Sci.* 2010;51:5260-5266.
8. Ikuno Y, Kawaguchi K, Nouchi T, Yasuno Y. Choroidal thickness in healthy Japanese subjects. *Invest Ophthalmol Vis Sci.* 2010;51:2173-2176.
9. Ding X, Li J, Zeng J, et al. Choroidal thickness in healthy Chinese subjects. *Invest Ophthalmol Vis Sci.* 2011;52:9555-9560.
10. Li XQ, Larsen M, Munch IC. Subfoveal choroidal thickness in relation to sex and axial length in 93 Danish university students. *Invest Ophthalmol Vis Sci.* 2011;52:8438-8441.
11. Wei WB, Xu L, Jonas JB, et al. Subfoveal choroidal thickness: the Beijing eye study. *Ophthalmology.* 2013;120:175-180.
12. Fujiwara T, Imamura Y, Margolis R, Slakter JS, Spaide RF. Enhanced depth imaging optical coherence tomography of the choroid in highly myopic eyes. *Am J Ophthalmol.* 2009;148:445-450.

13. Ikuno Y, Tano Y. Retinal and choroidal biometry in highly myopic eyes with spectral-domain optical coherence tomography. *Invest Ophthalmol Vis Sci.* 2009;50:3876-3880.
14. Nishida Y, Fujiwara T, Imamura Y, Lima LH, Kurosaka D, Spaide RF. Choroidal thickness and visual acuity in highly myopic eyes. *Retina.* 2012;32:1229-1236.
15. Flores-Moreno I, Lugo F, Duker JS, Ruiz-Moreno JM. The relationship between axial length and choroidal thickness in eyes with high myopia. *Am J Ophthalmol.* 2013;155:314-319.
16. Ho M, Liu DTL, Chan VCK, Lam DSC. Choroidal thickness measurement in myopic eyes by enhanced depth optical coherence tomography. *Ophthalmology.* 2013;120:1909-1914.
17. Grosvenor T, Scott R. Three-year changes in refraction and its components in youth-onset and early adult-onset myopia. *Optom Vis Sci.* 1993;70:677-683.
18. McBrien NA, Adams DW. A longitudinal investigation of adult-onset and adult-progression of myopia in an occupational group. Refractive and biometric findings. *Invest Ophthalmol Vis Sci.* 1997;38:321-333.
19. Zadnik K. Myopia development in childhood. *Optom Vis Sci.* 1995;74:603-608.
20. Saw SM, Katz J, Schein OD, Chew SJ, Chan TK. Epidemiology of myopia. *Epidemiol Rev.* 1996;18:175-187.
21. Fujiwara A, Shiragami C, Shirakata Y, Manabe S, Izumibata S, Shiraga F. Enhanced depth imaging spectral-domain optical coherence tomography of subfoveal choroidal thickness in normal Japanese eyes. *Jpn J Ophthalmol.* 2012;56:230-235.
22. Park KA, Oh SY. Analysis of spectral domain optical coherence tomography in preterm children: Retinal layer thickness and choroidal thickness profiles. *Invest Ophthalmol Vis Sci.* 2012;53:7201-7207.
23. Read SA, Collins MJ, Vincent SJ, Alonso-Caneiro D. Choroidal thickness in childhood. *Invest Ophthalmol Vis Sci.* 2013;54:3586-3593.
24. Ruiz-Moreno JM, Flores-Moreno I, Lugo F, Ruiz-Medrano J, Montero JA, Akiba M. Macular choroidal thickness in normal pediatric population measured by swept-source optical coherence tomography. *Invest Ophthalmol Vis Sci.* 2013;54:353-359.
25. Chakraborty R, Read SA, Collins MJ. Diurnal variations in axial length, choroidal thickness, intraocular pressure and ocular biometrics. *Invest Ophthalmol Vis Sci.* 2011;52:5121-5129.
26. Tan CS, Ouyang Y, Ruiz H, Sadda SR. Diurnal variation of choroidal thickness in normal, healthy subjects measured by spectral domain optical coherence tomography. *Invest Ophthalmol Vis Sci.* 2012;53:261-266.
27. Spaide RF, Koizumi H, Pozzoni MC. Enhanced depth imaging spectral-domain optical coherence tomography. *Am J Ophthalmol.* 2008;146:496-500.
28. Yanni SE, Wang J, Cheng CS, et al. Normative reference ranges for the retinal nerve fiber layer, macula, and retinal layer thicknesses in children. *Am J Ophthalmol.* 2013;155:354-360.
29. Buckhurst PJ, Wolffsohn JS, Shah H, Naroo SA, Davies LN, Berrow EJ. A new optical low coherence reflectometry device for ocular biometry in cataract patients. *Br J Ophthalmol.* 2009;93:949-953.
30. Chiu SJ, Li XT, Nicholas P, Toth CA, Izatt JA, Farsiu S. Automatic segmentation of seven retinal layers in SDOCT images congruent with expert manual segmentation. *Optics Express.* 2010;18:19413-19428.
31. Patel NB, Luo X, Wheat JL, Harwerth RS. Retinal nerve fiber layer assessment: area versus thickness measurements from elliptical scans centered on the optic nerve. *Invest Ophthalmol Vis Sci.* 2011;52:2477-2489.
32. Tunncliffe AH, Hirst JG. *Optics.* 2nd ed. London, UK: Association of British Dispensing Opticians; 1996:130-132.
33. Bennett AG. A method of determining the equivalent powers of the eye and its crystalline lens without resort to phakometry. *Ophthalmic Physiol Opt.* 1988;8:53-59.
34. Bland JM, Altman DG. Measuring agreement in method comparison studies. *Stat Methods Med Res.* 1999;8:135-160.
35. Rahman W, Chen FK, Yeoh J, Patel P, Tufail A, Da Cruz L. Repeatability of manual subfoveal choroidal thickness measurements in healthy subjects using the technique of enhanced depth imaging optical coherence tomography. *Invest Ophthalmol Vis Sci.* 2011;52:2267-2271.
36. Li LJ, Cheung CYL, Gazzard G, et al. Relationship of ocular biometry and retinal vascular calibre in preschoolers. *Invest Ophthalmol Vis Sci.* 2011;52:9561-9566.
37. Ouyang Y, Heussen FM, Mokwa N, et al. Spatial distribution of posterior pole choroidal thickness by spectral domain optical coherence tomography. *Invest Ophthalmol Vis Sci.* 2011;52:7019-7026.
38. Hayreh SS. Posterior ciliary artery circulation in health and disease. *Invest Ophthalmol Vis Sci.* 2004;45:749-757.
39. May CA. Non-vascular smooth muscle cells in the human choroid: distribution, development and further characterization. *J Anat.* 2005;207:381-390.
40. Nickla DL, Wallman J. The multifunctional choroid. *Prog Retin Eye Res.* 2010;29:144-168.
41. Summers JA. The choroid as a sclera growth regulator. *Exp Eye Res.* 2013;114:120-127.
42. Nickla DL, Wildsoet CF, Troilo D. Endogenous rhythms in axial length and choroidal thickness in chicks: implications for ocular growth regulation. *Invest Ophthalmol Vis Sci.* 2001;42:584-588.
43. Van Alphen GWHM. Choroidal stress and emmetropization. *Vision Res.* 1986;26:723-734.
44. Choong YF, Chen AH, Goh PP. A comparison of autorefractive and subjective refraction with and without cycloplegia in primary school children. *Am J Ophthalmol.* 2006;142:68-74.